Influence of effective stress and temperature on the creep behavior of a saturated compacted clayey soil

Zayad Kaddouri, Olivier Cuisinier, Farimah Masrouri

INFLUENCE OF EFFECTIVE STRESS AND TEMPERATURE ON THE CREEP BEHAVIOR OF A SATURATED COMPACTED CLAYEY SOIL

Zayad KADDOURI, Olivier CUISINIER, Farimah MASROURI

LEMTA, Laboratoire d'Énergétique et de Mécanique Théorique et Appliquée, (UMR 7563), CNRS - Université de Lorraine, 54505 Vandœuvre-lès-Nancy, France.

Corresponding author. E-mail address: zayad.kaddouri@univ-lorraine.fr

Abstract

The compacted clay barrier of shallow depth repositories for wastes would be subjected to temperature variations. Consequently, the hydro-mechanical properties of compacted clays could be progressively modified, and thus affect the performance of repositories. The influence of effective stress and temperature on the creep behavior of a saturated compacted clayey soil was experimentally investigated by performing a series of incremental loading creep tests using a temperature-controlled oedometer. Applied effective vertical stress varied from 10 to 1300 kPa within a large temperature range of 5°C to 70°C. The results showed that the compression and swelling indices appear not to be affected by temperature, whereas the yield stress decreases as the temperature increases. The secondary compression is time-dependent; creep strains decrease with time till reaching a stable value corresponding to a period of 10 days. The creep coefficient $C_{\alpha e}$ increases with the increase of the effective stress and temperature. Moreover, relationships between the creep coefficient $C_{\alpha e}$, incremental compression index C^*_c, effective stress and temperature were further analyzed. A linear relationship between $C_{\alpha e}$ and C^*_c was observed in the considered stress range and the ($C_{\alpha e}/C^*_c$) ratio appears to be temperature dependent. Finally, the main results were discussed and interpreted in the light of a suitable constitutive framework.

Keywords: compacted clay; oedometer; creep tests; effective stress; temperature.

Nomenclature

C	compression index
C_c^*	incremental compression index
C_s	swelling index
C_{s_L}	swelling index (loading slope before yield stress)
C_{s_UNL}	swelling index (unloading slope)
$C_{\alpha e}$	creep coefficient
CRS	constant rate of strain test
e	void ratio
e_0	initial void ratio
EOP	end of primary consolidation
IL_{EOP}	incremental loading till t_{EOP}
ILCr	creep incremental loading for 10 days
I_p	plasticity index
NCL	normal consolidation line
p_0^*	yield stress for saturated conditions
t	time
t_{EOP}	time equal to the end of primary consolidation
T	temperature
UNL_{EOP}	unloading till t_{EOP}
w_N	natural water content
w_L	liquid limit
w_P	plastic limit

α constant

ε_v vertical strain $(\Delta H / H_0)$

$\dot{\varepsilon}_v$ strain rate

κ swelling index corresponding to $C_s/\ln 10$

λ compression index corresponding to $C_c/\ln 10$

$\sigma_p^{'}$ yield stress

$\sigma_v^{'}$ effective vertical stress

1. Introduction

Compacted clays will be potentially used as engineering barriers for the disposal of waste at shallow depths due to their low permeability, high exchange capacity and retention properties[1]. These repositories will be submitted to cyclic changes of temperature due to climate variations over their service life (>10 000 years). These variations could affect the evolution of the hydro-mechanical properties, in particular the compressibility and the creep of these materials and consequently alter the long term performance of the repository. This study will be focused on the impact of temperature on the long-term behavior of compacted clays, and more specifically the impact of temperature variations on creep.

When a saturated clay soil is loaded one-dimensionally, its deformation occurs in two successive phases: (1) primary consolidation related to the dissipation of excess water pressure; and (2) secondary compression or creep, i.e., time-dependent deformation under constant effective stress. Two Hypotheses have been proposed by Ladd et al.[2]. Hypothesis A assumes that creep occurs only after the end of primary consolidation (EOP) and that the strain at EOP is the same in both in-situ (thick sample) and laboratory (thin sample) tests. In contrast, Hypothesis B assumes that creep occurs in the whole compression process and starts simultaneously with the primary consolidation, and that the strain at EOP depends on the sample thickness. To date, many models have been proposed to study creep behavior of soft soils (e.g., Šuklje[3]; Bjerrum[4]; Mesri and Goldewski[5]; Leroueil et al.[6]; Yin and Graham[7]; Grimstad et al.[8]). Detailed review of most constitutive models describing the creep behavior of soft clays has been done recently by Karim and Gnanendran[9]. In this context, Börgesson and Hernelind[10] investigated the canister settlement by modelling the shear creep effects in nuclear waste repositories using a

87 model based on Singh and Mitchell's[11] deviatoric creep formulation.

88 The creep coefficient $C_{\alpha e}$ is both time and stress dependent[5,12–17]. Suneel et al.[17] showed
89 that the creep strain increases with increasing effective stress in normally consolidated
90 state. In addition, the value of $C_{\alpha e}$ is related to other soil parameters (e.g. the natural water
91 content w_N, the compression index C_c and the effective stress $\sigma_v^{'}$), but the most common
92 correlation is the $C_{\alpha e}/C_c$ concept developed by Mesri and co-workers[5,18,19]. The $C_{\alpha e}/C_c$ is
93 considered a material constant, and is used together with the EOP e-log σ'_v curve to assess
94 the secondary compression behavior of any one soil[19]. Early laboratory work, in
95 particular, Walker and Raymond[20] highlighted a linear relationship between $C_{\alpha e}$ and C_c
96 on Leda clay over the entire applied stress range. This observation was confirmed by
97 many other researchers on various soils[18,19]. Later, it was found that $C_{\alpha e}$ and C_c increase
98 with the effective vertical stress, reach a maximum value at a stress slightly higher than
99 the yield stress, and then decrease and finally remain constant[14,17,21–23]. This divergence
100 about the relationship between $C_{\alpha e}$ and C_c could be related to the applied vertical stress
101 range values, i.e., it is more likely to observe a convex relationship at high vertical
102 stresses. Whatever is the shape of this relationship, the $C_{\alpha e}/C_c$ ratio was found to be
103 constant during the tests[5,17,20,23–25].

104 The temperature impact on the creep behavior of compacted soils has been considered in
105 a few number of studies. Based on oedometric creep tests results on Bryce clay at different
106 temperatures (from 5 to 50°C), Green[12] showed that the creep coefficient is both effective
107 stress and temperature dependent; the effect of temperature is more pronounced on $C_{\alpha e}$ at
108 low effective stress. Typically, under a constant effective stress of 96 kPa, $C_{\alpha e}$ varies by
109 37.5% when the temperature changes between 5 and 50°C[12]. A series of creep tests on a
110 clayey sulphide soils within a temperature range of 5-60°C showed that creep parameter

111 was dependent on temperature, the higher the temperature, the higher the creep
112 coefficient[26]. The creep behavior could also be evaluated by performing constant rate of
113 strain test (CRS)[27,15]. Leroueil et. al[15] suggested that the $C_{\alpha e}/C_c$ represents the same
114 behavior of the variation in the yield stress versus logarithmic cycle of time or strain rate,
115 i.e., $C_{\alpha e} / C_c = \Delta\log(\sigma_p^{'}) / \Delta\log(\dot{\varepsilon}_v) = \alpha$. Boudali et al.[28] and Marques et al.[29] conducted
116 CRS tests at various temperatures to investigate the influence of temperature on the strain
117 rate-yield stress relationship of a natural clays. They found approximately parallel slopes
118 of the logarithmic strain rate-yield stress relationship at different temperatures. The key
119 concern in this study is the impact of temperature on creep for compacted clays while
120 existing studies were primarily focused on natural sensitive clays that have a specific
121 microstructure and are highly cemented.

122 As the engineered barriers are made of compacted clayey soils, a correct assessment of
123 consolidation and creep behavior of the considered material is a fundamental necessity.
124 Investigation of the creep behavior dependency on changes in stress level and temperature
125 must be done. Therefore, this paper aims to investigate experimentally the variations of
126 $C_{\alpha e}$ under different effective vertical stresses at various temperatures of a saturated
127 compacted clayey soils. For this purpose, a temperature-controlled oedometer was used
128 to perform tests under a wide range of stress and temperature. The saturated compacted
129 samples were submitted to incremental loading oedometer creep tests, and the creep
130 coefficient was determined for each increment load. The results were analyzed with
131 $C_{\alpha e}/C_c$ concept.

2. Materials and methodology

2.1 Material

The study was performed on a compacted clayey soil from the East of France. The studied soil is composed of 35.9% clay minerals, 46.3% quartz, 9.9% Calcite, 4.3% Feldspar, 3% Plagioclase and 0.6% Gypsum. The clay minerals of the material, as determined by X-ray diffractometry, are kaolinite (38.4%), illite (26.5%), interstratified illite-smectite (26.2%), and chlorite (8.9%). A laser diffraction particle size analyzer (Malvern Mastersizer 2000®) was used to determine the particle size distributions of the soil. The soil is composed of approximately 72% of silt particles (smaller than 0.02 mm) and the remaining particles (25.5%) are smaller than 80 μm. Atterberg limits (AFNOR)[30] for studied clay were determined. The plastic limit (w_P) is 19.7%, the liquid limit (w_L) is 43.5% with plasticity index I_p=23.8%, and the specific gravity is 2.65. The standard Proctor curve showed that the maximum dry density is 1.74 Mg/m^3 at an optimum moisture content of 16.5% (AFNOR)[31]. The studied material is classified as lean clay, CL, according to the Unified Soil Classification System[32] and A2 according to the French standard for soil classification[33].

2.2 Sample preparation

For the sample preparation, the dry powder (< 400 μm) was carefully mixed and wetted with deaerated and demineralized to the standard optimum moisture content. The prepared soils were then stored in airtight bags for at least 24 hours for moisture content equilibration. Then, soil samples were statically compacted in greased stainless steel rings of the oedometer cells to the maximum dry density. The samples' dimensions are 50 mm in diameter and 10 ± 0.1 mm in height. The maximum compaction pressure reached is

1200 kPa. Initial void ratio determined in these conditions is 0,515 ± 0.008.

2.3 Compression creep tests

2.3.1 Testing device

An oedometer with temperature-control system was developed for conducting oedometer creep tests, and studying the combined effects of vertical stress and temperature on soils (Fig. 1). A compressed air pressure system was designed for the load application. The target vertical load was applied to the sample by air pressure through pressure regulator. The maximum corresponding vertical stress is 1300 kPa for 50 mm samples. Vertical displacement of the sample was measured using LVDT (linear variable differential transformer) sensors with an accuracy of 0.01 mm. The control of temperature was obtained using a climatic chamber. It allows for working at temperatures ranged from 5 to 100°C with a ± 0.7°C accuracy. The temperature is continuously measured and recorded during the test by a temperature sensor connected to the cell, near the soil sample. The system comprises also a volume/pressure controller to control the pore water pressure at the base of the sample. The sample is installed between two initially dry porous stones.

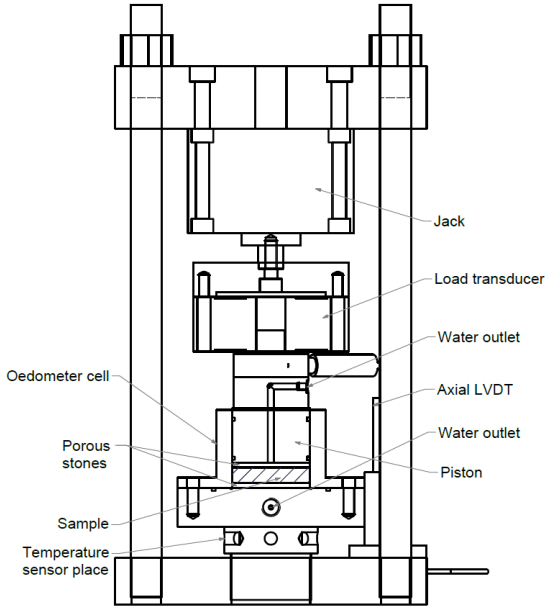

Fig. 1. Schematic drawing of the oedometer (placed in the temperature-controlled chamber).

2.3.2 Experimental procedures

The compacted sample with the confining ring was set up on the oedometer. An initial constant vertical stress of 10 kPa was applied to ensure the contact of loading piston with sample. Deaerated and demineralized water was then supplied to the sample through the porous element from the bottom to saturate the sample. A water pressure of 10 kPa was applied and maintained during the entire test at the base of the sample. The saturated samples were drained from the top (Fig. 1). An experimental procedure was established to check the material sample saturation level. Firstly, the injected water volume was measured as a linear function of time (over a long period of time) and secondly by measuring the water content of the sample at the end of the saturation phase (see Jarad[34]). The saturation phase was reached in seven days. Once, the vertical swelling deformation of the sample at this initial vertical stress and desired temperature was stabilized, the incremental loading was started. The ratio of change in applied vertical stress was limited to 0.5 times the previous vertical stress (AFNOR)[35]. Finally, at the end of the test, water content of the sample was measured and the degree of saturation was calculated and

188 confirmed to be equal to 100%, which indicates that the sample was fully saturated. In
189 the following sections, the end of the saturation phase was considered as the reference
190 initial state. It is also worth noting the concept of preconsolidation pressure considered in
191 this paper. Indeed, in its geological meaning, the preconsolidation pressure of a soil is
192 unique, constant and corresponds to its maximum overburden stress in its past stress
193 history. Otherwise, the preconsolidation pressure is assumed here as ‘‘yield stress’’ which
194 separates two domains: the overconsolidated domain (corresponding to low loads where
195 deformations are small and reversible) and the normally consolidated domain
196 (corresponding to high loads where deformations are more important and largely
197 irreversible). In this paper the Casagrande method is used to determine the yield stress
198 $\sigma_p^{'}$.

199 ***2.3.3 Experimental program***

200 In the context of shallow depth low activity radioactive waste disposals, the expected
201 effective vertical stresses vary between 360 and 500 kPa (corresponding to the depths
202 below 30 m), and the temperature values are supposed to be between 5 and 50°C[36,37]. To
203 respect this context, in this study, applied effective stresses were ranged between 10 and
204 1280 kPa, and temperature was imposed between 5-70°C. The experimental program
205 consists of three test series (Table 1):

206 • Series N°1: Tests TE1a to TE4b aim to determine the compressibility parameters (C_c,
207 C_s and $\sigma_p^{'}$) and to evaluate the temperature effect on these parameters. The samples
208 were mechanically loaded step by step up to a given stress (From 10 to 1280 kPa),
209 then the incremental unloading tests were performed. Each loading and unloading
210 step was maintained until the end of primary consolidation (t_{EOP}) was reached. The
211 tests conducted under 5, 50 and 70°C were repeated twice to check the repeatability

of the results. The void ratio e and vertical stress $\sigma_v^{'}$ (e-log $\sigma_v^{'}$) curves at different temperatures were determined.

- Series N°2: Tests TE5 to TE9 aim to determine the creep coefficient $C_{\alpha e}$ and to investigate the effective vertical stress and temperature impact on the creep coefficient $C_{\alpha e}$. The samples were incrementally loaded up to a given vertical stress (10, 16 and 30 kPa). Then, the creep incremental loading tests were performed for 10 days under different effective vertical stress (from 80 to 1280 kPa). At the end of 1280 kPa creep increment load, unloading increments were applied going back to 10 kPa. The incremental loading and unloading steps duration was equal to the t_{EOP}. Consolidation curves (e-log t) under different effective vertical stresses at various temperatures were determined. The applied temperatures are 5, 20, 50 and 70 ° C.
- Series N°3: Tests TE10 to TE15 performed at 20°C aim to complete the experimental data and to investigate the $C_{\alpha e}$ dependency on both time and effective vertical stress. The samples were incrementally loaded up to a given vertical stress (10, 16, 30 and 60 kPa). Then, the creep incremental loading tests were performed for 10 days under different effective vertical stress (from 80 to 640 kPa). $C_{\alpha e}$ was calculated at different effective vertical stress.

Table 1. List of tests in temperature-controlled oedometer cell.

Thermomechanical tests characteristics				Compressibility parameters			Creep coefficient
Series N°	Temperature (°C)	Applied vertical stress (kPa)	Step duration	C_c (-)	C_s (-)	σ'_p (kPa)	$C_{\alpha e}$ (-)
1	5 - 20 - 50 - 70	10 - 1280	t_{EOP}	✓	✓	✓	-
2	5 - 20 - 50 - 70	80 - 1280	10 days	-	-	-	✓
3	20	80 - 640	10 days	-	-	-	✓

3. Results

3.1 Void ratio-time relationship

A typical test result in terms of variation of void ratio with logarithm of time (e-log t) at a single loading step in the compression tests is presented in Fig. 2a. It shows the two phases of the compression process: (1) the primary consolidation, where excess pore pressure dissipated; and (2) the secondary compression, that corresponds to creep, i.e., deformation under constant effective stress due to internal soil structure rearrangement. The end of primary consolidation (EOP) is a point marking the transition between the two phases. It is defined graphically as the point of intersection of the tangent lines when void ratio is plotted against log time (Fig. 2a). In this framework, the secondary compression is assumed negligible during the primary consolidation and started at the EOP. It is quantified by the creep coefficient $C_{\alpha e}$ expressed by Eq. (1):

$$C_{\alpha e} = \frac{\Delta e}{\Delta \log(t)} \quad \textbf{(1)}$$

where Δe is the variation in void ratio and $\Delta \log t$ is the variation in time over one log cycle.

Fig. 2b shows the void ratio-time curves at different vertical stresses of sample TE5 (Temperature T=20°C). As shown in Fig. 2b, the slopes of void ratio-time curves decrease with time for vertical stress larger than 30 kPa, which means that $C_{\alpha e}$ of the studied samples is time-dependent. It can also be observed from Fig. 2b that $C_{\alpha e}$ varies with vertical stress, i.e. the creep strain increases consistently with increasing effective stress.

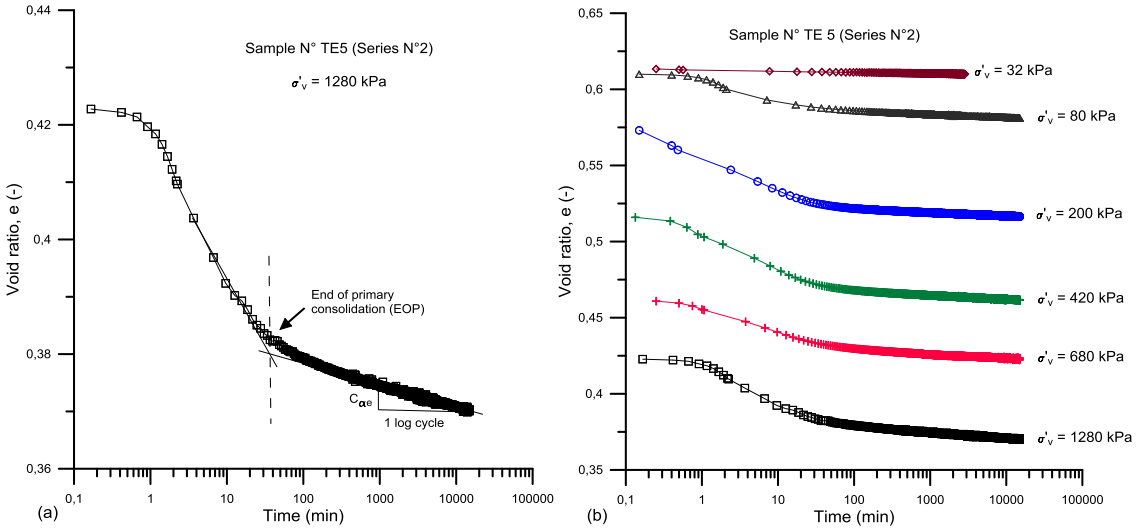

Fig. 2. Void ratio-time curves at 20°C: (a) void ratio-time curve at σ'$_v$=1280 kPa; (b) void ratio-time curves at different effective vertical stresses.

Fig. 3 shows the relationship between $C_{\alpha e}$ and the logarithm time during the secondary compression, where t_{EOP} corresponds to the time of the end of primary consolidation and consequently the start of the secondary compression. Depending on the shape of the $C_{\alpha e}$-log t curves under a given effective stress, it can be noted that $C_{\alpha e}$ decreases considerably with time at the beginning of the creep stage then stabilizes at $(t-t_{EOP})/(t_{EOP})$ close to 100, which corresponds to 14000 min. Therefore, 10 days are enough to determine $C_{\alpha e}$. Regarding the variation of $C_{\alpha e}$ with time during the secondary compression stage, it was observed that $C_{\alpha e}$ decreases in a more marked manner at 1280 kPa compared to 680 kPa. At 1280 kPa, $C_{\alpha e}$ decreases rapidly, during the first hour, from $9.5^{x}10^{-3}$ to $5.8^{x}10^{-3}$ followed by an intermediate period where $C_{\alpha e}$ continues to decrease and then reaches a final value of $3.8^{x}10^{-3}$. Whereas, at 680 kPa, $C_{\alpha e}$ decreases slowly from $5.9^{x}10^{-3}$ to $4.9^{x}10^{-3}$ followed by an intermediate period where $C_{\alpha e}$ continues to decrease and then reached a final value of $2.6^{x}10^{-3}$. These results confirm that $C_{\alpha e}$ is both time and stress dependent.

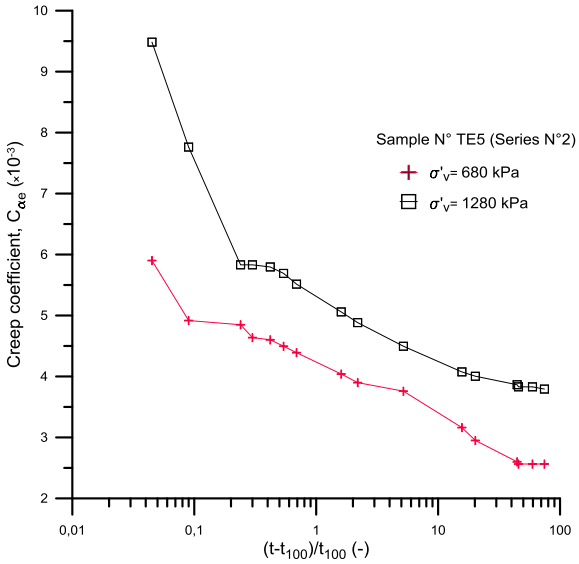

Fig. 3. Evolution of the creep coefficient $C_{\alpha\varepsilon}$ with normalized $(t-t_{EOP})/t_{EOP}$ at 20°C.

3.2 Void ratio-effective vertical stress behavior with temperature

Fig. 4 shows the relationship between the void ratio e and vertical stress σ'_v (e-log σ'_v) at different temperatures at t_{EOP}, including one typical e -log σ'_v curve at 20°C (Fig. 4a) and e-log σ'_v curves at different temperatures at t= t_{EOP}. Two compression tests were conducted under 5, 50 and 70°C following the same thermo-mechanical testing path. The two curves obtained under the same temperature are very similar demonstrating the good repeatability of the experiments (Fig. 4b and Table 2). The observed increase in void ratio at the initial vertical stress corresponds to the swelling deformation obtained when the sample is fully saturated (Fig. 4b). This increase is characterized by the swelling potential $\Delta H/H_0$, equivalent to $(\Delta e/ (1+e_0))$. This parameter was reduced at higher temperatures (Fig. 4b). For example, the swelling potential decreases from 6.9% at 20°C to 1.1% at 70°C. In the loading phase, the compressibility curves are characterized by a settlement which begins to appear only after the initial loading of 10 kPa during which the soil swells. In the unloading phase, the compressibility curves are characterized by highly accentuated slopes to which correspond high values of the swelling index. This behavior

is related to the swelling nature of the studied clay. Similar observation was stated by many researchers[38–41]. Fig. 4b also shows that, at constant temperature, the void ratio decreases with increasing vertical stress. Whereas, at constant vertical stress, the void ratio decreases with increasing temperature indicating that the soil becomes more compressible and the entire compression curve moves to the left.

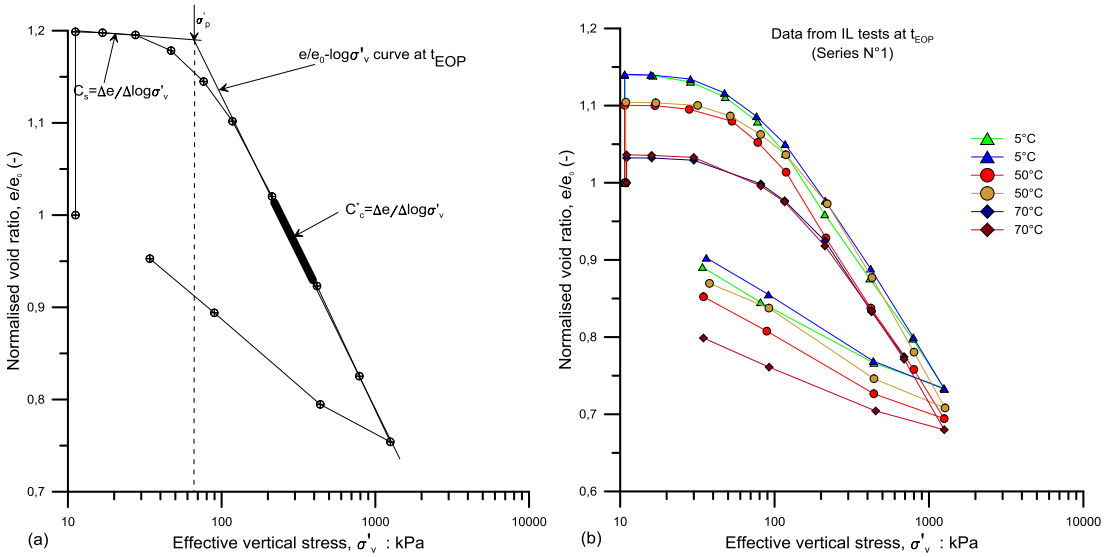

Fig. 4. Void ratio-effective vertical stress curves: (a) Void ratio-effective vertical stress curve at T=20°C at t_{EOP}; (b) Void ratio- stress curves at different temperatures at t_{EOP}.

3.2.1 Temperature effect on the swelling and compression indices

Based on the (e-log σ'_v) curves obtained at different temperatures at t_{EOP} (Fig. 4b), the compression index ($C_c = \Delta e/\Delta \log \sigma'_v$) and swelling index ($C_s = \Delta e/\Delta \log \sigma'_v$) were calculated as graphically illustrated in the Fig. 4a. The values of the compression index (C_c) and the swelling index (C_s), which are defined as the slope of the normal compression line and slope of the swelling line, respectively, are given in Table 2. Fig. 5a shows the variation of the compression and swelling indices with temperature. From the obtained experimental results, summarized in Table 2, it appears that the compression and swelling indices change very slightly with temperature. On average, the compression index (C_c)

and the swelling index (C_s) appear be about 0.161 and 0.007, respectively.

3.2.2 Temperature effect on the yield stress

The yield stress $\sigma_p^{'}$ of tested samples was evaluated using the Casagrande method as graphically represented in Fig. 4a. The determined yield stress for tested samples at 5, 20, 50 and 70°C are given in Table 2. A yield stress $\sigma_p^{'}$ – temperature relationship was plotted in Fig. 5b. It was found that as the soil temperature increases the yield stress σ'_p decreases. For example, the percentage of the decrease in yield stress $\sigma_p^{'}$ is 14.9% due to the temperature increase from 5 to 70°C. This corresponds to a negative hardening or softening of the soil.

Table 2. Effect of temperature on the $\Delta e/(1+e_0)$, C_c, C_{s_L}, C_{s_UNL}, and σ'_p.

T (°C)	$\Delta e/(1+e_0)$ (%)	C_c (-)	C_{s_L} (-)	C_{s_UNL} (-)	σ'_p (kPa)
5	4.79	0.163	0.008	0.059	68.4
5	4.84	0.155	0.011	0.066	67.9
20	6.70	0.172	0.005	0.072	66.5
20	6.85	0.160	0.013	0.067	65.1
50	3.43	0.161	0.006	0.059	62.6
50	3.51	0.162	0.005	0.058	62.0
70	1.10	0.158	0.004	0.047	58.0
70	1.29	0.158	0.004	0.047	58.0

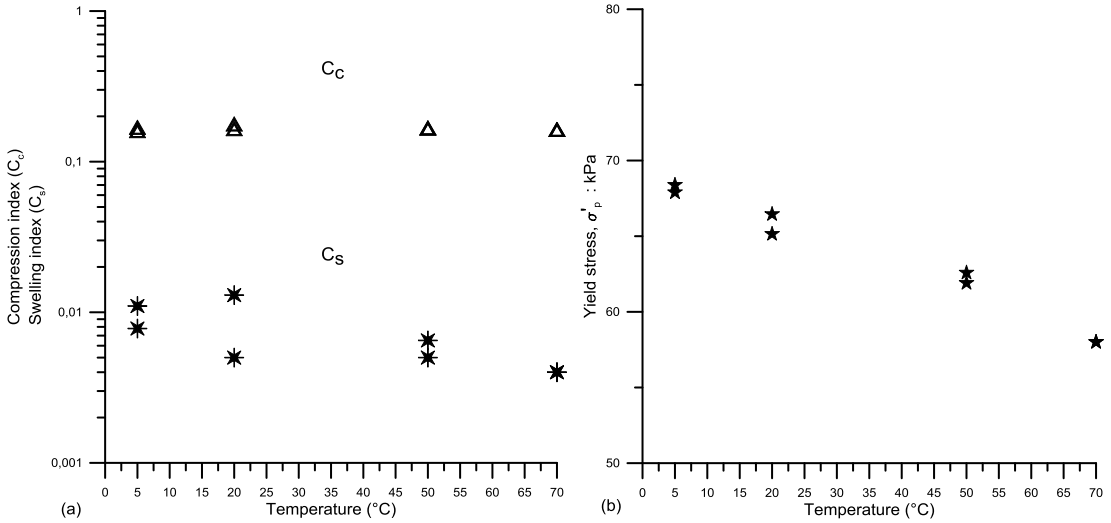

312

313 **Fig. 5. Effect of temperature on the compressibility parameters: (a) the swelling index (C_s), compression index**

314 **(C_c) and (b) the yield stress (σ'_p).**

315 ***3.3 Temperature and effective vertical stress effect on the creep coefficient***

316 To investigate the combined effect of temperature and effective vertical stress on the
317 secondary compression (creep) coefficient $C_{\alpha e}$, one-dimensional ILCr oedometer creep
318 tests were carried out on the studied material at 5, 20, 50 and 70°C (Table 1). In this study,
319 load increments prior to the creep ones were kept until the end of primary consolidation
320 is achieved. The duration for each creep load increment (ILCr) was more than ten days
321 under a constant effective vertical stress (Table 1). The values of $C_{\alpha e}$ were determined as
322 mentioned above in section 3.1.1 using Eq. (1). This approach was used to investigate $C_{\alpha e}$
323 for all samples. The evolution of the creep coefficient $C_{\alpha e}$ versus vertical stress at various
324 temperatures is depicted in Fig. 6. Accordingly, it can be seen that $C_{\alpha e}$ increases with
325 vertical stress and temperature increase, especially at higher effective vertical stress.
326 However, a scatter was observed in the initial stages of loading, which could be related
327 to the influence of stress level, void ratio, mechanical loading rate, loading mode and
328 loading interval. Regardless of this, the dependency of $C_{\alpha e}$ on the applied effective vertical
329 stress and temperature can be readily observed.

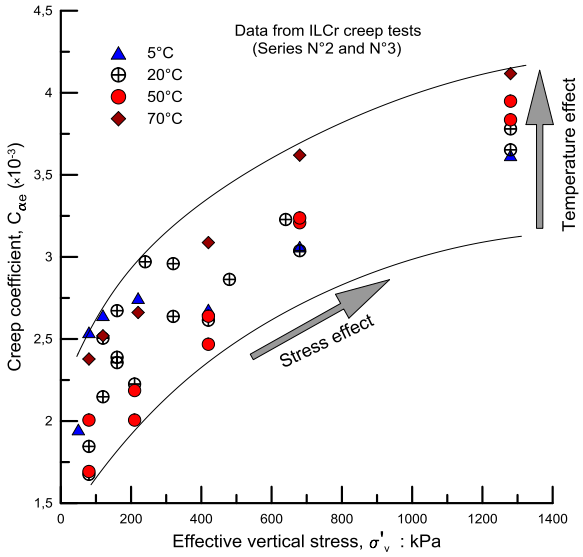

330

331 **Fig. 6. Secondary compression-effective vertical stress at different temperatures for all performed tests.**

332 To further investigate the effect of temperature, determined values of $C_{\alpha e}$ for the larger
333 level stresses are compared. Fig. 7 shows the variation range of creep coefficient $C_{\alpha e}$ with
334 temperature under higher effective stress corresponding to 680 kPa and 1280 kPa. An
335 increase in creep coefficient with increasing temperature can be observed. For example,
336 under the effective vertical stress of 1280 kPa, the increase percentage in $C_{\alpha e}$ is 13.6% as
337 the temperature increase from 5 to 70°C. These results confirmed that the $C_{\alpha e}$ is dependent
338 on the applied effective vertical stress and temperature.

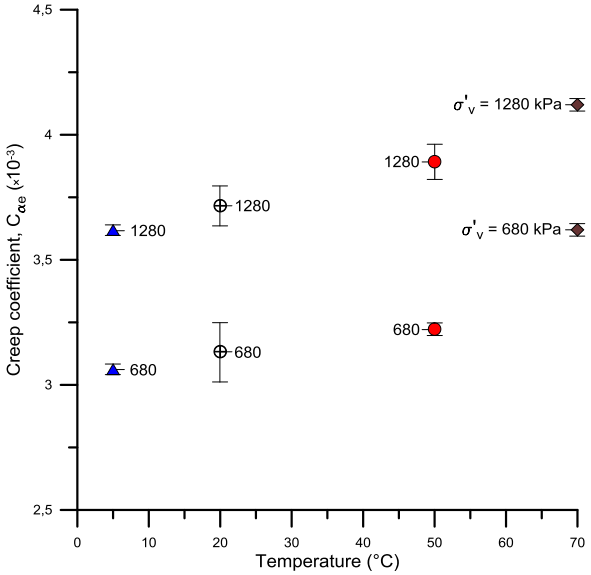

339

340 **Fig. 7. Variation range of the creep coefficient with temperature at σ'v =680 kPa and σ'v =1280 kPa.**

4. Discussion and analyses of results

The effect of temperature on the soil compressibility is first discussed. Moreover, the modification of the compressibility parameters with temperature is analyzed using the Cam-Clay Model. The main objective of the second part of the discussion section is to analyze the temperature impact on the creep coefficient in the framework of the $C_{\alpha e}/C_c$ concept proposed by Mesri and Goldewski[5].

4.1 Temperature effect on the soil compressibility

Based on the experimental results obtained in this study, temperature has appeared to modify very slightly the compression index (C_c) and swelling index (C_s). In the case of remolded illitic clay, by performing isothermal oedometer tests at various temperatures, Campanella and Mitchell[42] also indicated that the variations of (C_c) and (C_s) with temperature were negligible. This phenomenon has been subsequently confirmed by many other authors. Furthermore, all the tests performed at various temperatures showed an increase in the swelling index upon mechanical stress release when greater vertical stresses were reached. This behavior is commonly associated with the swelling nature of the clay[38–41]. Mohajerani et al.[43] and Crisci et al.[44] related the observed swelling index increase to the mechanical degradation of the material when subjected to high stresses and to various loading and unloading cycles.

The effect of temperature on the yield stress, which defines the limit between elastic and plastic domains, has been studied. The results obtained on compacted samples at 5, 20, 50 and 70°C showed a decrease of this parameter with increasing temperature. A decrease of this parameter with the temperature leads to a contraction of the elastic domain. As shown in Fig. 8, similar results were obtained on structured and natural soils by many

researchers[26,28,29,45–47]. This phenomenon could be related to the decrease in adsorbed water of clay particles. This reduction facilitates formation of mineral to mineral contacts because water acts as an elastic material between two clay particles and consequently produces plastic deformation and reduces the elastic domain[45,48].

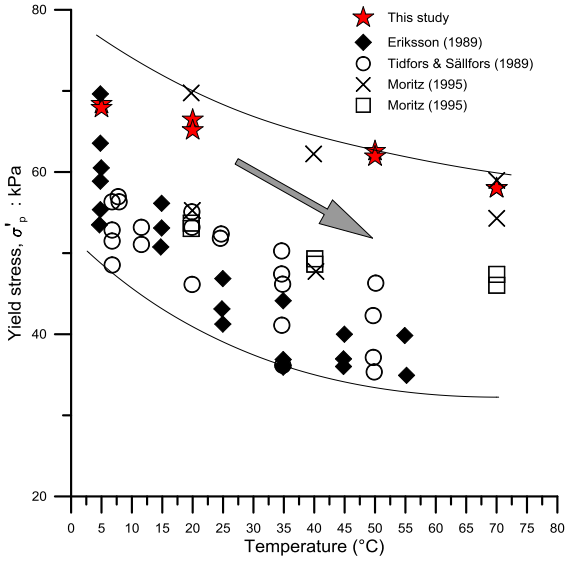

Fig. 8. Evolution of the yield stress with temperature: Comparison of the results obtained here with oedometric compression tests on different clayey materials (Eriksson 1989; Tidfors and Sällfors 1989; Moritz 1995).

Several relationships have been proposed in the literature to describe the evolution of the yield stress as a function of temperature (Laloui et Cekerevac[49]; Cui at al.[50]). Hueckel and Borsetto[51] were the first to propose an extension of the modified Cam-Clay Model to take into account the effect of temperature in the case of saturated soils:

$$p_0^*(T) = p_0^*(T_0) + \alpha_1 \Delta T + \alpha_2 \Delta T \left|\Delta T\right| \quad \textbf{(2)}$$

where p^*_0 is the yield stress in saturated state at a reference temperature (room temperature) T_0, T is the current temperature, $\Delta T = T\text{-}T_0$ stands for the temperature difference with respect to a reference temperature and α_1 and α_2 are the coefficients depending on thermal sensibility of the soil. By fitting experimental data, p^*_0, α_1 and α_2 were determined (Table 3). Afterwards, the compressibility behavior with temperature can be well simulated in the framework of the Cam-Clay Model using the equation (2)

and the calibrated parameters given in Table 3. In this model, the compression index (C_c) and the swelling index (C_s) are related to $\lambda(0)$ ($\lambda=C_c/\ln 10$) and κ ($\kappa = C_s/\ln 10$), respectively. These Cam Clay parameters are for volumetric strain in isotropic stress.

Table 3. Calibrated constitutive parameters.

C_c (-)	λ (0) (-)	C_s (-)	κ (-)	p^*_0 (kPa)	α_1 (-)	α_2 (-)
0.161	0.070	0.007	0.003	66.28	-0.0909	-0.0008

4.2 Temperature effect on the creep coefficient

A logarithmic function was used to fit oedometer tests data of void ratio against time after the primary consolidation (Fig. 2a). The results obtained on compacted samples at 5, 20, 50 and 70°C indicated an increase of $C_{\alpha e}$ at higher temperatures. For instance, under the effective vertical stress of 1280 kPa, the increase percentage in $C_{\alpha e}$ is 13.6% as the temperature increase from 5 to 70°C. These results revealed that the creep behavior of the tested compacted clayey soils is both stress and temperature dependent. The increase in creep coefficient at higher temperature could be explained by the reduction in viscosity of soil skeleton and pore water[52].

The Mesri and Goldewski[5] concept was adopted here to analyze the long term behavior of the studied clayey soil with temperature. For example, the value of $C_{\alpha e}$ at 1280 kPa, higher effective vertical stress, was chosen for each temperature-controlled oedometer creep test. The relationship between the maximum $C_{\alpha e}$ and C_c, defined as the slope of the NCL, for each of the three temperatures shows that the ratio $C_{\alpha e}/C_c$ varies in a narrow range from 0.022 to 0.026. Table 4 summarizes the values of the $C_{\alpha e}/C_c$ ratio at different temperatures. All the values of $C_{\alpha e}/C_c$ lie within the range of 0.025–0.075 proposed by Mesri and Godlewski[5] for a number of inorganic clays and silts. The results show also that the $C_{\alpha e}/C_c$ ratio increases with increasing temperature. As the compression index C_c changes slightly with temperature, the increase in the $C_{\alpha e}/C_c$ is due essentially to the

increase of the creep coefficient $C_{\alpha e}$ with increasing temperature. Then, it can be concluded that the $C_{\alpha e}/C_c$ ratio of the compacted soil is temperature dependent.

Table 4. Influence of temperature on the Cc, $C_{\alpha e}$ and the $C_{\alpha e}/C_c$ ratio at σ'_v = 1280 kPa.

T (°C)	C_c (-)	$C_{\alpha e}$ ($\times 10^{-3}$)	$C_{\alpha e}$ (-)	$C_{\alpha e}/C_c$ (-)
5	0.163	3.619	0.0036	0.022
20	0.172	3.780	0.0038	0.022
50	0.161	3.949	0.0040	0.025
70	0.158	4.112	0.0041	0.026

By examining closely the e-log σ'_v curves obtained at different temperatures, it appears that these curves are not perfectly linear during loading and unloading, especially for the initial loading stages (Fig. 4). Consequently, to further explore effects of temperature and effective vertical stress on the $C_{\alpha e}/C_c$ ratio, an incremental compression index C^*_c was defined by Eq. (3) as the change in void ratio during the load increment for the samples of series N°1. It should be pointed out that C^*_c differs from the compression index defined as the slope of the NCL. This approach was adopted by many other researchers[14,23,25].

$$C_c^* = \frac{\Delta e}{\Delta \log \sigma_v'} \quad \textbf{(3)}$$

where C^*_c is the incremental compression index; Δe is the change in void ratio over one load increment; $\Delta \sigma'_v$ is the change in stress over the same load increment correspondingly. It can be seen from the Fig. 9 that, during the initial loading stages, C^*_c increased almost linearly with effective vertical stress, then it increased more slowly and finally tended to be a constant value in the final loading stages. Fig. 9 also shows that, at higher vertical stress from 400 kPa to 1280 kPa, the incremental compression index C^*_c was not depended on temperature, particularly at 20 and 50°C.

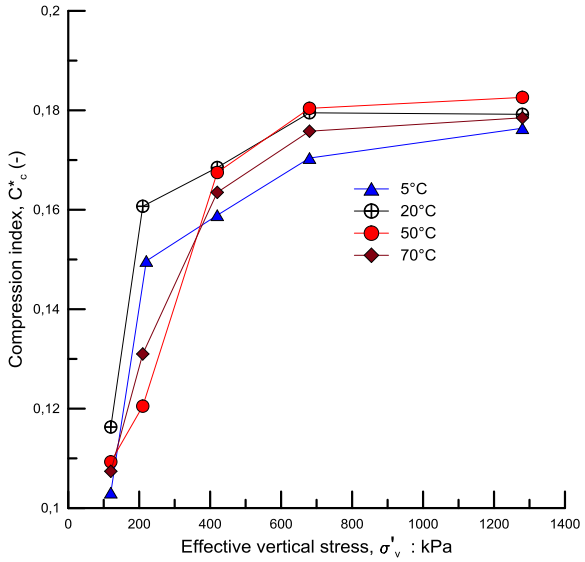

Fig. 9. Variation of C^*_c with applied vertical stress at different temperatures.

From the analysis mentioned above, it was shown that both the incremental compression index C^*_c and the secondary compression index $C_{\alpha e}$ are functions of effective vertical stress. The relationship between $C_{\alpha e}$ and C^*_c at different temperatures was investigated (Fig. 10). This evolution shows a limit value of C^*_c equal to 0.16, corresponding to an effective vertical stress of 420 kPa. The evolution of $C_{\alpha e}$ with C^*_c is quite constant at C^*_c values lower than 0.16 while $C_{\alpha e}$ increases in a more marked manner with C^*_c values higher than 0.16. Regarding the C^*_c values above the limit value, $C_{\alpha e}$ increases linearly with C^*_c (Fig. 10). The slopes of this linear increase of $C_{\alpha e}$ with C^*_c at 5, 20, 50 and 70°C are 0.0186, 0.0179, 0.0182 and 0.0209, respectively. It was found that the $C_{\alpha e}/ C^*_c$ ratio increases with temperature increase (Fig. 11). Fig. 11 shows also the evolution of $C_{\alpha e}/ C_c$ ratio with temperature.

Based on the obtained results, it can be concluded that the concept of $(C_{\alpha e}/C^*_c)$ ratio may also be applied to the used material in this study in the range of C^*_c higher than 0.16. On conclusion, in the light of these findings, the ratio of $C_{\alpha e}/C^*_c$ could be assumed temperature dependent for the studied compacted soil.

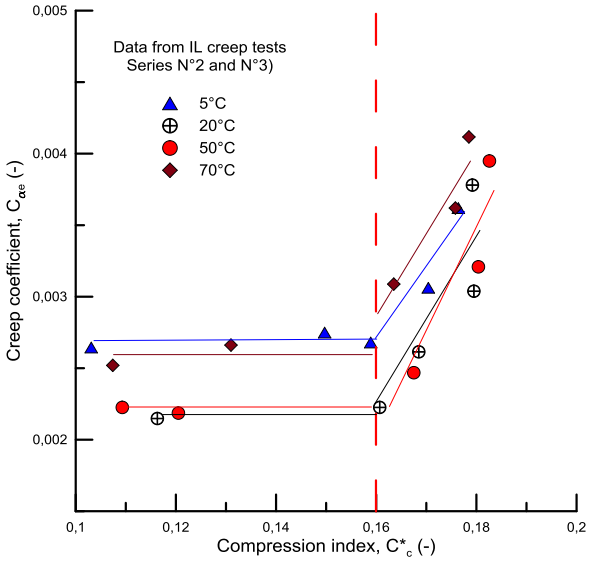

441

442 **Fig. 10. Evolution of $C_{\alpha e}$ versus C^*_c.**

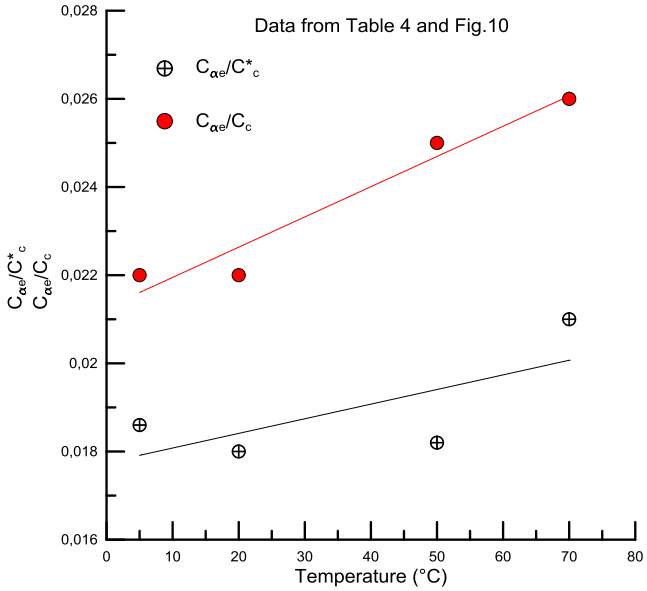

443

444 **Fig. 11. $C_{\alpha e}$ / C_c and $C_{\alpha e}$ / C^*_c versus temperature.**

445 ## 5. Conclusions

446 The influence of effective stress and temperature on the creep behavior of a saturated
447 compacted clayey soil was experimentally investigated by performing a series of
448 temperature-controlled oedometer tests. The e –log σ'_v and e-log t curves were plotted to
449 determine the swelling index C_s, compression index C_c, incremental compression index

C^*_c, and creep coefficient $C_{\alpha e}$. Moreover, different relations such as $C_{\alpha e}$-σ'_v, $C_{\alpha e}$-(t-t_{EOP})/t_{EOP}, $C_{\alpha e}$-C_c, and $C_{\alpha e}$-C^*_c were analyzed. Conclusions can be drawn as follows:

1. The swelling potential ($\Delta e/(1+e_0)$) is affected by temperature, it decreases as temperature increases.
2. The compression index (C_c) and swelling index (C_s) vary slightly in the range of studied temperatures.
3. The yield stress (σ'_p) is temperature dependent, it was found that as the soil temperature increases the yield stress σ'_p decreases.
4. The creep coefficient $C_{\alpha e}$ and the incremental compression index C^*_c are both stress-dependent and increase almost linearly with the effective stress increase.
5. The creep coefficient $C_{\alpha e}$ increases with increasing temperature, especially at higher effective vertical stresses. Whereas, the incremental compression index C^*_c could be considered independent of temperature.
6. The slope of the $C_{\alpha e}$ - C^*_c depends on a limit value of C^*_c: for C^*_c<0.16 a constant evolution of $C_{\alpha e}$ with C^*_c is observed, while for C^*_c>0.16 $C_{\alpha e}$ increases linearly with C^*_c. In addition, this linear relationship appears to be dependent on temperature, with a slightly higher ($C_{\alpha e}/C^*_c$) ratio at higher temperatures due to the increase of $C_{\alpha e}$ with increasing temperature.

Furthermore, the results of this work allowed information to be gathered for better understanding the creep behavior of compacted clayey soils as a function of effective vertical stress and temperature. The obtained data will be also used to model the behavior of structures made up of compacted soils under the effect of thermal variations in the long term.

Acknowledgment

The authors would like to thank ANDRA for providing the soil used in this study and fruitful discussions and expertise.

References

1. Lerouge, C. *et al.* A deep alteration and oxidation profile in a shallow clay aquitard: Example of the Tégulines Clay, East Paris Basin, France. *Geofluids* **2018,** 1–20 (2018).

2. Ladd, C. C., Foott, R., Ishihara, K., Schlosser, F., & Poulos, H. G. Stress-deformation and strength characteristics. *State-of-the-Art Report, Proc. 9th Int. Conf. SMFE* **2,** 421–494 (1977).

3. Šuklje, L. The analysis of the consolidation process by the isotaches method. in *Proceedings of the 4th International Conference on soil mechanics and foundation engineering* 200–206 (1957).

4. Bjerrum, L. Engineering geology of Norwegian normally-consolidated marine clays as related to settlements of buildings. *Géotechnique* **17,** 81–118 (1967).

5. Mesri, G. & Godlewski, M. Time and stress compressibility interrelationship. *J. Geotech. Geoenvironmental Eng.* **103,** 417–430 (1977).

6. Leroueil, S., Kabbaj, M., Tavenas, F. & Bouchard, R. Stress–strain–strain rate relation for the compressibility of sensitive natural clays. *Géotechnique* **35,** 159–180 (1985).

7. Yin, J.-H. & Graham, J. Elastic viscoplastic modelling of the time-dependent stress-strain behaviour of soils. *Can. Geotech. J.* **36,** 736–745 (1999).

8. Grimstad, G., Degago, S. A., Nordal, S. & Karstunen, M. Modeling creep and rate effects in structured anisotropic soft clays. *Acta Geotech.* **5,** 69–81 (2010).

9. Karim, M. R. & Gnanendran, C. T. Review of constitutive models for describing the time dependent behaviour of soft clays. *Geomech. Geoengin. an Int. J.* **9,** 36–51 (2014).

10. Börgesson, L. & Hernelind, J. Canister displacement in KBS-3V. A theoretical study (No. SKB-TR-06-04). *Swedish Nuclear Fuel and Waste Management Co. 43p*. (2006).

11. Singh, A. Mitchell, J. K. General stress-strain-time function for soils. in *Soil Mechanics and Foundation Division, vol. 94,* 21–46 (1968).

12. Green, W. J. The influence of several factors on the rate of secondary compression of soil. Master's thesis. Missouri-Holla, Holla, Missouri. 49p. (1969).

13. Tavenas, F., Leroueil, S., Rochelle, P. L., & Roy, M. Creep behaviour of an undisturbed lightly overconsolidated clay. *Can. Geotech. J.* **15,** 402–423. (1978).

14. Graham, J., Crooks, J. H. A. et Bell, A. L. Time effects on the stress – strain behaviour of natural soft clays. *Géotechnique* **33,** 327–340 (1983).

15. Leroueil, S., Kabbaj, M., Bouchard, R. & Tavenas, F. Stress—strain—strain rate relation for the compressibility of sensitive natural clays. *Géotechnique* **35,** 159–180 (1985).

16. Olson, R. E. Secondary consolidation. Advanced Soil Mechanics -Secondary Effects. *Departement of Construction Engineering Chaoyang University of Technology. 99-119*. (1989).

17. Suneel, M., Park, L. K. & Im, J. C. Compressibility characteristics of Korean marine clay. *Mar. Georesources Geotechnol.* **26,** 111–127 (2008).

18. Mesri, G., Choi, Y. K. The uniqueness of the end-of- primary (EOP) void ratio-effective stress relationship. *Proc. 11th ICSMFE, San Fr.* **2,** 587–590 (1985).

19. Mesri, G. & Castro, A. Cα/Cc concept and K0 during secondary compression. *J. Geotech. Eng.* **113,** 230–247 (1987).

20. Walker, L. K. & Raymond, G. P. The prediction of consolidation rates in a cemented clay. *Can. Geotechncial J.* **5,** 192–216. (1968).

21. Mesri, G., Stark, T. D., Ajlouni, M. A., & Chen, C. S. Secondary compression of peat with or without surcharging. *J. Geotech. Geoenvironmental Eng.* **135,** 411–421 (1997).

22. Walker, L. K. Secondary settlement in sensitive clays: Discussion. *Can. Geotech. J.* **6,** 219–222. (1969).

23. Powell, J. S., Take, W. A., Siemens, G. & Remenda, V. H. Time-dependent behaviour of the Bearpaw Shale in oedometric loading and unloading. *Can. Geotech. J.* **49,** 427–441 (2012).

24. Feng, T. W., Lee, J. Y. & Lee, Y. J. Consolidation behavior of a soft mud treated with small cement content. *Eng. Geol.* **59,** 327–335 (2001).

25. Deng, Y. F., Cui, Y. J., Tang, a. M., Li, X. L. & Sillen, X. An experimental study on the secondary deformation of Boom clay. *Appl. Clay Sci.* **59–60,** 19–25 (2012).

26. Eriksson, L. G. Compression properties of sulphide soils–Influence from time and

temperature, a laboratory study. Licentiate thesis, Luleå University of Technology, Sweden. 151p. (1992).

27. Leroueil, S. The isotache approach. Where are we 50 years after its development by Professor Šuklje? (2006 Prof. Šuklje's Memorial Lecture). in *Proceedings of the 13th Danube-European Conference on Geotechnical Engineering; Ljubljana, Vol. 1*, 55–88 (2006).

28. Boudali, M., Leroueil, S., et Murthy, B. S. Viscous behaviour of natural clays. *Proc. 13th Int. Conf. Soil Mech. Found. Eng. New Delhi, India* **1,** 411–416 (1994).

29. Marques, M. E. S., Leroueil, S. & Soares de Almeida, M. de S. Viscous behaviour of St-Roch-de-l'Achigan clay, Quebec. *Can. Geotech. J.* **41,** 25–38 (2004).

30. AFNOR. NF P94-051 - Sols: reconnaissance et essais: Détermination des limites d'Atterberg - Limite de liquidité à la coupelle - Limite de plasticité au rouleau. *Assoc. Française Norm. Paris, Fr.* (1993).

31. AFNOR. NF P94-093 - Sols: Reconnaissance et essais : Détermination des références de compactage d 'un matériau. Essai Proctor Normal - Essai Proctor Modifié. *Assoc. Française Norm. Paris, Fr.* (1999).

32. ASTM. Standard practice for classification of soils for engineering purposes (Unified Soil Classification System) (p. 12). West Conshohocken. PA: ASTM International. (2006).

33. GTR. Réalisation des remblais et des couches de forme. *Paris Lab. Cent. des Ponts Chaussées.* (p. 102). (2000).

34. Jarad, N. Temperature impact on the consolidation and creep behaviour of

compacted clayey soils. Thèse de doctorat. Université de Lorraine. France. 183p. (2016).

35. AFNOR. XP P94-090-1 - Sols : reconnaissance et essais - Essai oedométrique - Partie 1 : essai de compressibilité sur matériaux fins quasi saturés avec chargement par paliers. *Assoc. Française Norm. Paris, Fr.* (1997).

36. Andra. Etude des scenarios de gestion a long terme des dechets de faible activite massique a vie longue. *Document technique. 56p.* (2012).

37. Andra. Projet de stockage de déchets radioactifs de faible activité massique à vie longue (FA-VL). *Rapport d'étape 2015. 66p.* (2015).

38. Khemissa, M., Mekki, L. & Mahamedi, A. Laboratory investigation on the behaviour of an overconsolidated expansive clay in intact and compacted states. *Transp. Geotech.* **14,** 157–168 (2018).

39. Picarelli, L. & Di Maio, C. Deterioration processes of hard clays and clay shales. *Geol. Soc. London, Eng. Geol. Spec. Publ.* **23,** 15–32 (2010).

40. Weimin, M. Y., Zhang, F., Chen, B., Chen, Y. G., Wang, Q., & Cui, Y. J. Effects of salt solutions on the hydro-mechanical behavior of compacted GMZ01 Bentonite. *Environ. Earth Sci.* **72,** 2621–2630 (2014).

41. Tang, A. M. & Cui, Y. J. Experimental study on hydro-mechanical coupling behaviours of highly compacted expansive clay. *J. Rock Mech. Geotech. Eng.* **2,** 39–43 (2010).

42. Campanella, R. G. & Mitchell, J. K. Influence of temperature variations on soil behavior. *J. Soil Mech. Found. Div, ASCE* **94,** 709–734 (1968).

43. Mohajerani, M. *et al.* Oedometric compression and swelling behaviour of the Callovo-Oxfordian argillite. *Int. J. Rock Mech. Min. Sci.* **48,** 606–615 (2011).

44. Crisci, E., Ferrari, A., Giger, S., & Laloui, L. One Dimensional Consolidation of Opalinus Clay from Shallow Depth. *Adv. Lab. Test. Model. Soils Shales. Springer, Cham*, 338–344 (2017).

45. Tidfors, M., & Sallfors, G. Temperature effect on preconsolidation pressure. *Geotech. Test. Journal, GTJODJ* **12,** 93–97 (1989).

46. Moritz, L. Geotechnical Properties of Clay at Elevated Temperatures. Report N° 47.*Swedish Geotechnical Institute (SGI), Linköping, Sweden. 69p*. (1995).

47. Cekerevac, C., Laloui, L. & Vulliet, L. Dependency law for thermal evolution of preconsolidation pressure. in *Proceedings of the 8th International Symposium on Numerical Models in Geomechanics. Lisse: Swets & Zeitlinger* 687–692 (2002).

48. Shariatmadari, N. & Saeidijam, S. The effect of elevated temperature on compressibility and swelling of bentonite-sand mixtures. *Electron. J. Geotech. Eng.* **16 B,** 137–146 (2011).

49. Laloui, L. & Cekerevac, C. Numerical simulation of the non-isothermal mechanical behaviour of soils. *Comput. Geotech.* **35,** 729–745 (2008).

50. Cui, Y. J., Sultan, N., & Delage, P. Thermomechanical model for saturated clays. *Can. Geotech. J.* **37,** 607–620 (2000).

51. Hueckel, T. & Borsetto, M. Thermoplasticity of saturaed clays: constitutive equations. *J. Geotech. Eng.* **116,** 1765–1777 (1990).

52. Akagi, H., & Komiya, K. Constant rate of strain consolidation properties of clayey soil at high temperature. in *Proc. Int. Symp. Compression and Consolidation of Clayey Soils–IS–Hiroshima.* **95,** 3–8 (1995).

List of Tables

Table 1. List of tests in temperature-controlled oedometer cell. 12

Table 2. Effect of temperature on the $\Delta e/(1+e_0)$, C_c, C_{s_L}, C_{s_UNL}, and σ'_p. 17

Table 3. Calibrated constitutive parameters. 22

Table 4. Influence of temperature on the Cc, $C_{\alpha e}$ and the $C_{\alpha e}/C_c$ ratio at σ'_v = 1280 kPa. 23

List of Figures

Fig. 1. Schematic drawing of the oedometer (placed in the temperature-controlled chamber). 10

Fig. 2. Void ratio-time curves at 20°C: (a) void ratio-time curve at σ'_v=1280 kPa; (b) void ratio-time curves at different effective vertical stresses. 14

Fig. 3. Evolution of the creep coefficient $C_{\alpha e}$ with normalized $(t-t_{EOP})/t_{EOP}$ at 20°C. 15

Fig. 4. Void ratio-effective vertical stress curves: (a) Void ratio-effective vertical stress curve at T=20°C at t_{EOP}; (b) Void ratio- stress curves at different temperatures at t_{EOP}. 16

Fig. 5. Effect of temperature on the compressibility parameters: (a) the swelling index (C_s), compression index (C_c) and (b) the yield stress (σ'_p). 18

Fig. 6. Secondary compression-effective vertical stress at different temperatures for all performed tests. 19

Fig. 7. Variation range of the creep coefficient with temperature at σ'_v =680 kPa and σ'_v =1280 kPa. 19
Fig. 8. Evolution of the yield stress with temperature: Comparison of the results obtained here with oedometric compression tests on different clayey materials (Eriksson 1989; Tidfors and Sällfors 1989; Moritz 1995). 21
Fig. 9. Variation of C^*_c with applied vertical stress at different temperatures. 24
Fig. 10. Evolution of $C_{\alpha e}$ versus C^*_c. 25
Fig. 11. $C_{\alpha e}$ / C_c and $C_{\alpha e}$ / C^*_c versus temperature. 25